A Switching Diffusion Model for Lifetime Estimation in Randomly-Varying Environments

John A. Flory[1] and Jeffrey P. Kharoufeh[2]
Department of Industrial Engineering
University of Pittsburgh
1048 Benedum Hall
3700 O'Hara Street
Pittsburgh, PA 15261 USA

and

Nagi Z. Gebraeel[3]
H. Milton Stewart School of Industrial and Systems Engineering
Georgia Institute of Technology
Atlanta, GA 30332 USA

Final version appears in
IIE Transactions, 46 (11), pp. 1227–1241, 2014.

Abstract

We present a switching diffusion model for estimating the useful lifetime of a component that operates in a randomly-varying environment. The component's degradation process is unobservable; therefore, a signal of degradation is observed to estimate the environment parameters using a Markov chain Monte Carlo (MCMC) statistical procedure. These parameter estimates serve as key inputs to an analytical stochastic model that approximates the first passage time of the degradation process to a critical threshold. Several numerical examples involving simulated and real degradation data are presented to illustrate the quality of these approximations.

[1]Ph: (412) 624-9830; Email: jhnflory@gmail.com
[2]Corresponding author. Ph: (412) 624-9832; Email: jkharouf@pitt.edu
[3]Ph: (404) 894-0054; Email: nagi.gebraeel@isye.gatech.edu

1 Introduction

Assessing the lifetime of a component that operates in a randomly-varying environment is a challenging problem, particularly when the specific attributes of the environment are not known *a priori*, or cannot be easily discerned. The general problem we present here is primarily motivated by wind turbine applications wherein critical components (e.g., bearing, gears, shafts, etc.) are subjected to randomly-varying loads due to uncertain and time-varying wind speeds. The primary purpose of this paper is to develop a general, stochastic modeling framework within which the evolution of a related degradation signal can be estimated in order to characterize the environment and assess the expected lifetime of the component. To this end, we present a hybrid stochastic modeling framework to approximate the degradation process from an observed degradation signal that is characterized as a switching diffusion process. Using the signal observations, the environment parameters are estimated using a Markov chain Monte Carlo (MCMC) statistical procedure. These parameters are the key inputs of an analytical stochastic model that approximates the first passage time of the associated degradation process to a critical threshold value. The techniques developed herein are unique in that they impose fairly mild assumptions, are based solely on the observation of a real signal, and are applicable in a variety of contexts.

Conventional failure models typically assume that components operate in environments that are either time-invariant or do not significantly influence degradation as noted in [11]. Those models that include a time-varying environment generally fall into one of two broad categories: (1) proportional hazard models (PHM); or (2) stochastic degradation models. Originally introduced by Cox [13], the flexible PHM has been widely used to relate the hazard function of a component's lifetime to environmental conditions as in [4, 26, 32, 36]. Myers [40] presented a model in which the hazard function is a quadratic, time-varying function of the environment. Likewise, Gamerman [17] studied dynamic operating conditions in which the hazard function is piecewise exponential. Other extensions and applications of proportional hazard models that assume a deterministic environment include [33, 39, 46, 50, 52]. These models assume the evolution of the covariate (namely the environment condition) is known – an assumption that can be rather restrictive. Banjevic et al. [4] assumed the environment covariate is driven by a Markov process and used an approximation scheme to estimate the failure time distribution, which is expressed in a complex integral form. Computational issues associated with their approach were addressed by Banjevic and Jardine [3], who developed a general numerical method to approximate the failure time distribution. Similar approximation techniques were applied in [22] wherein the authors used a hidden Markov model to characterize the unobservable degradation status. Zhao et al. [53] discussed condition-based inspection policies for systems subject to random shocks whose amplitudes are driven by a Markovian environment. For an extensive review of other related models, the reader is referred to the comprehensive survey paper by Si et al. [44].

The second broad category of approaches encompasses a class of stochastic degradation models that attempt to characterize the evolution of degradation (or a signal of degradation) using classical

stochastic models, e.g., Brownian motion processes or general diffusions, Lévy processes, Markov reward models, and random coefficient models. Some representative samples include [14, 19, 20, 27]. These types of models are appealing because they often lead to tractable distribution functions for the component lifetime. Doksum and Hóyland [14] used Brownian motion with a stress-dependent drift parameter in accelerated life testing to derive the failure time distribution using a certain transformation; a similar approach was employed by Whitmore and Schenkelberg [51]. Gebraeel and Pan [20] extended the model in [14] to include shocks occurring at environment transition epochs. Such models consider environments that evolve deterministically and have been widely used in accelerated life testing ([37, 48]) and biomedical engineering ([33]) applications. Most relevant to our work are those models that consider randomly-varying environments, a sampling of which are surveyed by Singpurwalla [45]. Generally speaking, the influence of the environment on degradation takes one of two forms: (1) random shocks that increase or decrease the degradation instantaneously; and (2) random variations in the rate of degradation due to the environment's evolution. Esary et al. [15] first considered a system subject to random shocks that arrive according to a Poisson process; their model was later extended in [2, 16]. Lemoine and Wenocur [35] examined the lifetime distribution of a system under dynamic stress that was modeled as a time-nonhomogeneous Poisson process whose rate parameter is driven by a shot-noise process. Igaki et al. [25] analyzed the lifetime of a system under environmental conditions that evolve as a Markov renewal shock process.

Approaches in which the degradation rate is driven by the environment's evolution include Çinlar [9, 10] who analyzed an additive process in which the environment is Markovian, and the degradation evolves as an increasing Lévy process. Özeckici and Soyer [41] studied a Markov-modulated Bernoulli process for which the success probability – the probability that a periodically-inspected component survives a given inspection period – is determined by a Markov process. Using Bayesian inference techniques, they estimated the model parameters, depending on the observability of the process. Kharoufeh et al. [27, 28] examined a problem in which a component degrades linearly at a rate that depends on the state of a continuous-time Markov chain (CTMC) and derived explicit double Laplace transform expressions for the distribution function and moments of the component lifetime. That work was extended in [29] to include homogeneous Poisson shocks, each of which induces a random amount of damage to the component. In [30], a model with Markov-modulated degradation rates and Poisson shock intensities was studied. Both transient and asymptotic reliability indices were obtained therein. Kharoufeh et al. [31] extended the model of [27] to the case when the environment is a semi-Markov process.

As in [27], we assume the component operates in a randomly-varying environment so that the true rate of degradation depends on the state of the environment, which is assumed to evolve as a CTMC (an assumption that can easily be relaxed). The primary objective of this paper is to develop a novel stochastic and statistical modeling framework wherein the environment process that drives degradation can be inferred from an observed signal of degradation that evolves over time.

Specifically, our aim is to estimate the environment process parameters from the signal's evolution in order to compute the distribution function and moments of the signal's first passage time to a critical threshold. To this end, we first describe how the degradation model of [27] can be related to a switching diffusion model whose drift parameter is modulated by a CTMC. The advantage of the switching diffusion framework is that it can be used to characterize the evolution of many types of degradation processes, and a Markov chain Monte Carlo procedure can be exploited to estimate the parameters of the modulating environment from real signal observations, facilitating approximations of the first passage time distribution and moments. To validate the techniques, we compare these approximated first passage times with those generated by simulation models, as well as those observed in real degradation data sets. In both cases, the procedure is shown to characterize the degradation processes remarkably well, even when the model assumptions are violated.

The remainder of the paper is organized as follows. Section 2 briefly reviews a stochastic model that forms the basis of our procedure and describes its relationship to the switching diffusion model of the degradation signal. Section 3 describes in detail a Markov chain Monte Carlo procedure for converting real signal observations into environment parameter estimates and lifetime assessments. In Section 4, we validate these procedures using both simulated and real degradation data. Finally, we conclude the paper in Section 5 by discussing the strengths and weaknesses of our approach, as well as directions for future work.

2 Model Description

Consider a component that is placed into service at time $t = 0$ in new condition. Gradually, the component degrades due to normal usage and the influence of its operating environment. Once the component's cumulative degradation level exceeds a (deterministic) critical threshold x ($x > 0$), it is declared to be failed. Let $Z(t)$ be the state of the operating environment at time t. The process $\mathcal{Z} = \{Z(t) : t \geq 0\}$ is the *stochastic environment process*, and its state space is a finite set $\mathcal{S} = \{1, \ldots, \ell\}$, where ℓ is the number of distinct environment states. This model, originally proposed and analyzed in [27, 28], assumes that $\mathcal{Z}$ is an irreducible, time-homogeneous CTMC on $\mathcal{S}$ with infinitesimal generator matrix $\boldsymbol{Q} = [q_{ij}]$, $i, j \in \mathcal{S}$. It is important to note that the CTMC assumption can be relaxed to analyze non-Markovian environments [31]; however, we present the Markovian case here to elucidate the main concepts. Let $\{Z_n : n \geq 0\}$ be the discrete-time Markov chain (DTMC) embedded at transition epochs of $\mathcal{Z}$, i.e., Z_n is the state of $\mathcal{Z}$ just after the nth transition, $n \geq 1$, and let $\boldsymbol{P} = [p_{ij}]$, $i, j \in \mathcal{S}$, be its transition probability matrix. We assume the existence of a real-valued function $r : \mathcal{S} \to (0, \infty)$ such that whenever $Z(t) = i \in \mathcal{S}$, the component degrades linearly at a unique, constant rate r_i ($r_i > 0$).

The states of $\mathcal{Z}$ can represent either (i) the actual ambient environment in which the component resides and operates (e.g., ambient air temperature, humidity, exposure to sunlight, etc.) and/or

(ii) the various operational settings of the equipment (e.g., operating speed or load). Potential interactions between environmental conditions and operational settings are not precluded from influencing degradation; therefore, the finite set of governing environment states $\mathcal{S}$ is composed of all unique combinations of the environmental conditions and operational settings. For example, if the component is subject to two different temperature regimes, denoted t_- and t_+, and two different operating speeds, denoted v_- and v_+, the state space of the governing environment is the Cartesian product of $\{t_-, t_+\}$ and $\{v_-, v_+\}$; that is, $\mathcal{S} = \{(t_-, v_-), (t_-, v_+), (t_+, v_-), (t_+, v_+)\}$, and $\ell = |\mathcal{S}| = 4$. While in many applications, it may be possible to observe environment or operating conditions, it is often difficult to establish a realistic mapping between these conditions and their associated degradation rates. Therefore, ℓ must be inferred from real degradation (or degradation signal) observations. Because the degradation rates are distinguishable, the states of $\mathcal{S}$ may be completely ordered such that $i < j$ if $r_i < r_j$, $i, j \in \mathcal{S}$. Let the row vector $\boldsymbol{r} = (r_1, r_2, \ldots, r_\ell)$ contain these ℓ ordered rates and set $\boldsymbol{R}_d = \text{diag}(\boldsymbol{r})$.

Next, we briefly review a model for the cumulative degradation process originally described in [27]. Denote by $X(t)$ the cumulative degradation of the component up to time t given by

$$X(t) = X(0) + \int_0^t r_{Z(u)} \mathrm{d}u,$$

where $X(0) = 0$ with probability 1 (w.p. 1). To ensure the process is well-defined, it is assumed that

$$\int_0^t \left| r_{Z(u)} \right| \mathrm{d}u < \infty \text{ w.p. 1.}$$

The component's random lifetime is the first passage time

$$T(x) = \inf\{t > 0 : X(t) \geq x\},$$

which is finite w.p. 1 (see Kharoufeh et al. [29]). The strict positivity of the degradation rates r_i, $i \in \mathcal{S}$, ensures that the sample paths of $\{X(t) : t \geq 0\}$ are piecewise linear and monotone increasing w.p. 1. Moreover, for $x > 0$ and $t \geq 0$, the events $\{X(t) < x\}$ and $\{T(x) > t\}$ are equivalent, so the first passage time $T(x)$ can be analyzed via $X(t)$. Let $F(x,t) \equiv \mathbb{P}(T(x) \leq t) = 1 - \mathbb{P}(X(t) \leq x)$ denote the cumulative distribution function (c.d.f.) of the component's lifetime. As proved in [29, 30], the Laplace-Stieltjes transform (LST) of $F(x,t)$, with respect to the spatial variable x, is

$$\widetilde{F}(u,t) \equiv \int_0^\infty e^{-ux} F(\mathrm{d}x, t) = 1 - \boldsymbol{\alpha} \exp\left[(\boldsymbol{Q} - u\,\boldsymbol{R}_d)t\right] \boldsymbol{e}, \quad u > 0, \tag{1}$$

where $\boldsymbol{\alpha} = [\mathbb{P}(Z(0) = i)]_{i \in \mathcal{S}}$ is the environment's initial distribution, $\exp[\boldsymbol{A}]$ denotes matrix exponentiation of a square matrix $\boldsymbol{A}$, and $\boldsymbol{e}$ is an $\ell \times 1$ vector of ones. Furthermore, if $m^n(x) \equiv \mathbb{E}(T^n(x))$ denotes the nth moment of the lifetime distribution, then $\widetilde{m}^n(u)$, the LST of $m^n(x)$ with respect to the spatial variable x, is given by

$$\widetilde{m}^n(u) \equiv \int_0^\infty e^{-ux} \mathrm{d}m^n(x) = n!\, \boldsymbol{\alpha}(u\boldsymbol{R}_d - \boldsymbol{Q})^{-n} \boldsymbol{e}, \;\; n \geq 1. \tag{2}$$

Now, if ℓ, $\boldsymbol{\alpha}$, $\boldsymbol{r}$, and $\boldsymbol{Q}$ are known, or if they can be estimated from observed data (cf. [28]), the component's full (or residual) lifetime distribution and moments can be obtained by inverting (1) and (2), respectively, for any failure threshold $x > 0$ using the numerical inversion algorithms of Abate and Whitt [1]. That is,

$$F(x,t) = \mathcal{L}^{-1}\{u^{-1}\widetilde{F}(u,t)\}, \tag{3}$$

$$m^n(x) = \mathcal{L}^{-1}\{u^{-1}\widetilde{m}^n(u)\}, \quad n \geq 1, \tag{4}$$

where $\mathcal{L}^{-1}$ is the inverse Laplace transform operator.

Besides the transient results of (1) and (2), the asymptotic behavior of $\{T(x) : x > 0\}$ has been studied in [29, 30]. In the asymptotic regime (as $x \to \infty$), the expected lifetime can be approximated using Theorem 1, which is adapted from Proposition 1 and Theorem 3 of [30].

Theorem 1 *As $x \to \infty$,*

$$\frac{T(x)}{x} \to \frac{1}{\pi_s \boldsymbol{r}'} \text{ w.p. 1} \quad \text{and} \quad \frac{\mathbb{E}[T(x)]}{x} \to \frac{1}{\pi_s \boldsymbol{r}'}, \tag{5}$$

where π_s is the stationary distribution of $\boldsymbol{Q}$.

Realistically, it might be difficult (or impossible) to directly observe the cumulative degradation of a component. A quintessential example is the case of a critical wind turbine component (e.g., a bearing, rotating shaft, or a gear) that is housed possibly hundreds of feet above the ground in the wind turbine's nacelle. For such components, sensors can provide proxy signals of degradation (e.g., vibration or acoustic signals). These signals are typically noisy due to sensor measurement error or corruption of the transmitted signal (cf. [18, 19, 20, 38]). Accounting for the uncertainty of such measurements is vitally important when assessing the true health of the component. The partial observability of $X(t)$ suggests the need for an alternative modeling framework.

Let $Y(t)$ denote a degradation signal observation at time t, and let $\{Y(t) : t \geq 0\}$ be the *signal process* for short. For reasons that will become apparent later, we assume $\{Y(t) : t \geq 0\}$ evolves as a switching diffusion process (SDP). A SDP generalizes a standard diffusion process by allowing the drift parameter and/or diffusion coefficient to be modulated by an external stochastic process $\{Z(t) : t \geq 0\}$ that evolves on a finite state space. The SDP satisfies the general stochastic differential equation

$$\mathrm{d}Y(t) = \mu(Y(t), Z(t)) + \xi(Y(t), Z(t))\,\mathrm{d}B(t), \tag{6}$$

where $\mu(Y(t), Z(t))$ is the drift function, $\xi(Y(t), Z(t))$ is the (non-negative) diffusion function, $\{B(t) : t \geq 0\}$ is a standard Brownian motion process, and $\{Z(t) : t \geq 0\}$ is typically a finite CTMC. The relevance of the SDP to the degradation process $\{X(t) : t \geq 0\}$ is now explained. If the functions μ and ξ are restricted so that

$$\mu(Y(t), Z(t)) = r_{Z(t)}\mathrm{d}t,$$

and $\xi(Y(t), Z(t)) = \sigma$ for each $t \geq 0$, then $Y(t)$ satisfies the stochastic differential equation

$$\mathrm{d}Y(t) = r_{Z(t)}\mathrm{d}t + \sigma \mathrm{d}B(t), \tag{7}$$

where σ ($\sigma \geq 0$) is a time-invariant diffusion coefficient. For each $t \geq 0$, the unique solution to the stochastic differential equation, with initial condition $Y(0) = 0$ w.p. 1, is

$$\begin{aligned} Y(t) &= \int_0^t r_{Z(u)}\mathrm{d}u + \sigma B(t) \\ &\equiv X(t) + \sigma B(t). \end{aligned} \tag{8}$$

That is, $\{Y(t) : t \geq 0\}$ can be viewed as the superposition of $\{X(t) : t \geq 0\}$ with a noise process whose time-dependent variance is $\sigma^2\, t$. We see immediately that

$$\mathbb{E}[Y(t)] = \mathbb{E}\left[X(t) + \sigma B(t)\right] = \mathbb{E}[X(t)], \quad t \geq 0.$$

Here is the crux of our approach: Because $X(t)$ cannot be directly observed to estimate ℓ, $\boldsymbol{Q}$, and $\boldsymbol{r}$, we instead construct estimators $\hat{\ell}$, $\widehat{\boldsymbol{Q}}$, and $\widehat{\boldsymbol{r}}$ via the evolution of the degradation signal $\{Y(t) : t \geq 0\}$. By observing $Y(t)$, we can exploit techniques for inferring the parameters of switching diffusion models (see [34]) to estimate the unknown environment process $\mathcal{Z}$ and, subsequently, to estimate $X(t)$ via $Y(t)$. Of particular interest to our work here are Markov chain Monte Carlo inference procedures that are tailored specifically for switching diffusion processes (cf. [7, 23, 24, 34]). The next section describes how we estimate the environment parameters $\boldsymbol{Q}$, $\boldsymbol{r}$ and $\ell = |\mathcal{S}|$, as well as the first passage times of $\{X(t) : t \geq 0\}$, via the signal process $\{Y(t) : t \geq 0\}$.

3 Estimation Procedure

In this section, we describe the means by which to adapt a Markov chain Monte Carlo (MCMC) procedure of Leichty and Roberts [34] to obtain estimates of $\boldsymbol{Q}$, $\boldsymbol{r}$, and σ, denoted by $\widehat{\boldsymbol{Q}}$, $\widehat{\boldsymbol{r}}$, and $\widehat{\sigma}$, respectively, from discrete observations of $\{Y(t) : t \geq 0\}$. Additionally, we describe a Bayesian information criterion (BIC) statistic to estimate ℓ and a forward-filtering-backward-smoothing (FFBS) algorithm to estimate the mean path of the signal Y.

3.1 MCMC Procedure to Estimate $\boldsymbol{Q}$, $\boldsymbol{r}$ and σ

Let $\mathcal{T} = \{t_0, t_1, t_2, \ldots, t_N\}$ denote a set of $N+1$ discrete observation times, where $t_0 \equiv 0$ and $t_N \equiv T < T'_x \equiv \inf\{t > 0 : Y(t) \geq x\}$, and define $\mathcal{Y} = \{Y(0), Y(t_1), \ldots, Y(T)\}$ as the set of signal observations at times in $\mathcal{T}$, where $Y(0) = 0$ w.p. 1. We construct a piecewise-linear function $Y_c(t)$ to approximate $Y(t)$ on $[0, T]$ such that (i) $Y_c(t_j) = Y(t_j)$, $j = 0, 1, \ldots, N$, and (ii) $\mathrm{d}Y_c(t)/\mathrm{d}t$ is defined for all t except for $t_j \in \mathcal{T}$ and is constant within intervals $(t_{j-1}, t_j]$, $j = 1, 2, \ldots, N$. Our aim is to estimate the expected lifetime of the component using estimates of the environment parameters $(\boldsymbol{Q}, \boldsymbol{r}, \ell)$ obtained from the data $\mathcal{Y}$ and used in equations (1) and (2).

Initially, let us assume that $\mathcal{Z}$ has ℓ states for some $\ell \in \mathbb{N}$. Let $\widehat{Z}(t)$ be an estimate of $Z(t)$ at time $t \in [0,T]$, and $\widehat{z} \equiv \{\widehat{Z}(t) : t \in [0,T]\}$ be the estimated sample path of $\mathcal{Z}$. The procedure consists of sequentially sampling from, and updating, the conditional densities of $\boldsymbol{r}|\boldsymbol{Q},\widehat{z},\mathcal{Y}$, $\boldsymbol{Q}|\widehat{z},\boldsymbol{r},\mathcal{Y}$, and $\widehat{z}|\boldsymbol{r},\boldsymbol{Q},\mathcal{Y}$ denoted by $f_{\boldsymbol{r}}(\boldsymbol{r}|\boldsymbol{Q},\widehat{z},\mathcal{Y})$, $f_{\boldsymbol{Q}}(\boldsymbol{Q}|\widehat{z},\boldsymbol{r},\mathcal{Y})$, and $f_{\widehat{z}}(\widehat{z}|\boldsymbol{r},\boldsymbol{Q},\mathcal{Y})$, respectively. A single iteration of the algorithm includes the following steps:

1. Randomly sample $\widehat{\boldsymbol{r}}_{v+1} \sim f_{\boldsymbol{r}}(\boldsymbol{r}|\widehat{\boldsymbol{Q}}_v,\widehat{z}_v,\mathcal{Y})$,
2. Randomly sample $\widehat{\boldsymbol{Q}}_{v+1} \sim f_{\boldsymbol{Q}}(\boldsymbol{Q}|\widehat{z}_v,\widehat{\boldsymbol{r}}_{v+1},\mathcal{Y})$,
3. Randomly sample $\widehat{z}_{v+1} \sim f_{\widehat{z}}(\widehat{z}|\widehat{\boldsymbol{r}}_{v+1},\widehat{\boldsymbol{Q}}_{v+1},\mathcal{Y})$,

where $\widehat{\boldsymbol{r}}_v$, $\widehat{\boldsymbol{Q}}_v$, and $\widehat{z}_v$ denote the estimates of $\boldsymbol{r}$, $\boldsymbol{Q}$ and $\mathcal{Z}$, respectively, at the vth iteration, $v = 0,1,2,\ldots$. The diffusion coefficient σ^2 is estimated *a priori* using a simple estimator of the quadratic variation of a diffusion process,

$$\widehat{\sigma}^2 = \frac{1}{N}\sum_{j=1}^{N}\frac{[Y(t_j) - Y(t_{j-1})]^2}{t_j - t_{j-1}}.$$

Although the estimator $\widehat{\sigma}^2$ is biased (since it includes the variance induced by the switching process), it is used only as an initial input of the MCMC procedure and remains constant throughout the procedure. Prior densities and hyperparameters for $\widehat{\boldsymbol{r}}_0$, $\widehat{\boldsymbol{Q}}_0$, and $\widehat{z}_0$ must be specified. Assume the prior density of $\widehat{\boldsymbol{r}}_0$ is a constrained, multivariate normal density and obtain $\widehat{\boldsymbol{r}}_0 = \left(\hat{r}_1^{(0)} \;\; \hat{r}_2^{(0)} \;\; \cdots \;\; \hat{r}_\ell^{(0)}\right)$ by randomly sampling $\widehat{\boldsymbol{r}}_0$ from a density proportional to

$$\phi\left(\mathbf{0},\boldsymbol{\Delta}\right)\mathbb{I}\left(\hat{r}_1^{(0)} < \hat{r}_2^{(0)} < \cdots < \hat{r}_\ell^{(0)}\right),$$

where $\phi\left(\mathbf{0},\boldsymbol{\Delta}\right)$ is the multivariate normal probability density function (p.d.f.) with mean $\mathbf{0}$ (an $\ell \times 1$ vector of zeros), and covariance matrix $\boldsymbol{\Delta} \equiv \text{diag}(\delta_1,\delta_2,\ldots,\delta_\ell)$. Typically, one can set $\delta_i = 3\widehat{\sigma}^2$ for all $i \in \mathcal{S}$ so that the prior distribution of $\widehat{\boldsymbol{r}}_0$ is relatively diffuse. For the prior distribution of $\widehat{\boldsymbol{Q}}_0$, it is assumed that the off-diagonal elements are independent, exponentially distributed random variables whose rates are determined by a hyperparameter β. Specifically, to initialize $\widehat{\boldsymbol{Q}}_0 = [\widehat{q}_{ij}^{(0)}]$, for each $i,j \in \mathcal{S}$ such that $j \neq i$, sample $\widehat{q}_{ij}^{(0)} \sim \text{Exp}(\beta)$ and compute $q_{ii}^{(0)}$ by normalizing the ith row of $\widehat{\boldsymbol{Q}}_0$, i.e.,

$$\widehat{q}_{ii}^{(0)} = \sum_{j:j\neq i}\widehat{q}_{ij}^{(0)},$$

where $\beta^{-1} = T/3$. The estimated sample path $\widehat{z}$ is initialized by generating $\widehat{z}_0$ via simulation using $\widehat{\boldsymbol{Q}}_0$, where $\mathbb{P}(\widehat{Z}(0) = i) = 1/|\mathcal{S}|$ for all $i \in \mathcal{S}$. Extensive empirical testing indicates that the procedure converges faster when $\widehat{z}_0$ is initialized so that it allows for relatively few transitions. Assigning $\beta^{-1} = T/3$ ensures that the average holding time in each state is relatively long so that the total number of transitions in $\widehat{z}_0$ is small.

Next, we describe the conditional densities $f_{\boldsymbol{r}}(\boldsymbol{r}|\boldsymbol{Q},\widehat{z},\mathcal{Y})$, $f_{\boldsymbol{Q}}(\boldsymbol{Q}|\widehat{z},\boldsymbol{r},\mathcal{Y})$, and $f_{\widehat{z}}(\widehat{z}|\boldsymbol{r},\boldsymbol{Q},\mathcal{Y})$. Define for each $i \in \mathcal{S}$ the constants

$$a_i = \frac{1}{\widehat{\sigma}^2}\int_0^T \mathbb{I}(Z(u)=i)\mathrm{d}Y(u),$$
$$b_i = \frac{1}{\widehat{\sigma}^2}\int_0^T \mathbb{I}(Z(u)=i)\mathrm{d}u + \delta_i^{-2}.$$

Intuitively, a_i is a proxy for the cumulative change of $Y(t)$ while the environment is in state i, and b_i is a proxy for the environment's total occupation time in state i during $[0,T]$. Define the $\ell \times 1$ vector $\boldsymbol{\mu} = (a_1/b_1 \;\; a_2/b_2 \;\cdots\; a_\ell/b_\ell)$ and the $\ell \times \ell$ diagonal matrix $\boldsymbol{\Sigma} = \mathrm{diag}(b_1^{-1}, b_2^{-1}, \ldots, b_\ell^{-1})$. The element a_i/b_i estimates the state-i degradation rate r_i for $i \in \mathcal{S}$. The conditional density function $f_{\boldsymbol{r}}(\boldsymbol{r}|\boldsymbol{Q},\widehat{z},\mathcal{Y})$ is a constrained multivariate normal density, i.e.

$$f_{\boldsymbol{r}}(\boldsymbol{r}|\boldsymbol{Q},\widehat{z},\mathcal{Y}) \sim N(\boldsymbol{\mu},\boldsymbol{\Sigma}) \quad \text{s.t.} \quad r_1 < r_2 < \cdots < r_\ell. \tag{9}$$

For the conditional density of $\boldsymbol{Q}$, it is assumed that the off-diagonal elements are independent, Gamma-distributed random variables. For each $i,j \in \mathcal{S}$ (with $j \neq i$), denote by ϑ_{ij} the number of environment transitions from state i to j in $\widehat{z}$ during $[0,T]$, let $\alpha_{ij} \equiv \vartheta_{ij} + 1$, and

$$\gamma_i^{-1} \equiv \int_0^T \mathbb{I}(Z(u)=i)\mathrm{d}u + \beta, \;\; i \in \mathcal{S}.$$

Let

$$f_{\boldsymbol{Q}}(\boldsymbol{Q}|\widehat{z},\boldsymbol{r},\mathcal{Y}) \sim \prod_{j:j\neq i} g\left(\alpha_{ij},\gamma_i^{-1}\right) \tag{10}$$

subject to the constraint

$$q_{ii} = -\sum_{j\neq i} q_{ij} \;\text{ w.p. } 1, \quad i \in \mathcal{S},$$

where $g(a,b)$ is the Gamma density function with shape parameter a and scale parameter b. The parameter α_{ij} can be viewed as a proxy for the total number of transitions from state i to j in $[0,T]$, and γ_i^{-1} is a surrogate for the total cumulative time spent in environment state i. For $j \neq i$, the mean of q_{ij} is $\alpha_{ij}\gamma_i^{-1}$, which is approximately equal to the maximum likelihood estimate (MLE) of q_{ij} given by $(\alpha_{ij}-1)/(\gamma_i - \beta)$ (see [6]). Lastly, $f_{\widehat{z}}(\widehat{z}|\boldsymbol{r},\boldsymbol{Q},\mathcal{Y})$ is a nonstandard density function of the form

$$f_{\widehat{z}}(\widehat{z}|\boldsymbol{r},\boldsymbol{Q},\mathcal{Y}) \propto \prod_{j:j\neq i} \vartheta_{ij} \exp\left[\frac{1}{\widehat{\sigma}^2}\int_0^T \sum_{i=1}^{\ell} \mathbb{I}(Z(u)=i)\mathrm{d}Y(u)\right]$$
$$\times \exp\left[\int_0^T \sum_{i=1}^{\ell}\left[\mathbb{I}(Z(u)=i)\left(-q_{ii} + \frac{r_i^2}{2\widehat{\sigma}^2}\right)\right]\mathrm{d}u\right]. \tag{11}$$

In a given iteration, proposed values $\widehat{\boldsymbol{r}}'$ and $\widehat{\boldsymbol{Q}}'$ for $\widehat{\boldsymbol{r}}$ and $\widehat{\boldsymbol{Q}}$ are generated from (9) and (10), respectively. The candidate $\widehat{\boldsymbol{r}}'$ is always accepted with probability 1, but $\widehat{\boldsymbol{Q}}'$ is accepted with

probability

$$\alpha(\widehat{\boldsymbol{Q}}, \widehat{\boldsymbol{Q}}') = 1 \wedge \frac{\pi_{\widehat{\boldsymbol{Q}}'}(\hat{Z}(0))}{\pi_{\widehat{\boldsymbol{Q}}}(\hat{Z}(0))},$$

where $\pi_{\widehat{\boldsymbol{Q}}'}(i)$ and $\pi_{\widehat{\boldsymbol{Q}}}(i)$, $i \in \mathcal{S}$, are the ith elements of the stationary distributions of CTMCs with respective generator matrices $\widehat{\boldsymbol{Q}}'$ and $\widehat{\boldsymbol{Q}}$. Obtaining $\widehat{\boldsymbol{r}}$ and $\widehat{\boldsymbol{Q}}$ from (9) and (10) is relatively straightforward; however, obtaining $\widehat{z}$ from (11) is more involved and requires modification using one of three procedures. The procedures are dubbed the *independence sampler*, *the refinement sampler*, and *the birth-death sampler*, where p_{is}, p_{rs}, and p_{bd} denote the samplers' respective selection probabilities such that $p_{is} + p_{rs} + p_{bd} = 1$. The process of updating $\widehat{z}$ is a Metropolis-Hastings (MH) step. That is, a sampler is randomly selected to propose a realization of the estimated CTMC sample path, denoted by $\widehat{z}'$, and the path $\widehat{z}'$ is accepted with probability $\alpha_{is}(\widehat{z}, \widehat{z}')$, $\alpha_{rs}(\widehat{z}, \widehat{z}')$, or $\alpha_{bd}(\widehat{z}, \widehat{z}')$ for the independence, refinement, and birth-death samplers, respectively. If $\widehat{z}'$ is accepted, $\widehat{z}_{v+1} = \widehat{z}'$; otherwise, $\widehat{z}_{v+1} = \widehat{z}$. For detailed descriptions of these three samplers, the reader is referred to Leichty and Roberts [34].

To obtain the final estimates of $\boldsymbol{r}$ and $\boldsymbol{Q}$, we appeal to the MCMC convergence result (cf. Gelfand and Smith [21]) $(\widehat{\boldsymbol{r}}_v, \widehat{\boldsymbol{Q}}_v, \widehat{z}_v) \xrightarrow{d} \pi(\boldsymbol{r}, \boldsymbol{Q}, \mathcal{Z})$ as $v \to \infty$, where $\xrightarrow{d}$ denotes weak convergence, and $\pi(\boldsymbol{r}, \boldsymbol{Q}, \mathcal{Z})$ is the stationary distribution of the Markov chain $\{(\widehat{\boldsymbol{r}}_v, \widehat{\boldsymbol{Q}}_v, \hat{z}_v) : v \geq 0\}$. Therefore, to obtain $\widehat{\boldsymbol{r}}$ and $\widehat{\boldsymbol{Q}}$, the sampled vectors $\widehat{\boldsymbol{r}}_v$ and the off-diagonal elements of $\widehat{\boldsymbol{Q}}_v$ are averaged after a burn-in period. Although implementation of the MCMC procedure requires that the number of environment states ℓ be known *a priori*, it is possible to estimate ℓ using the MCMC procedure in concert with the classical Bayesian information criterion (BIC) statistic [43]. Let $\widehat{\ell}$ denote the BIC estimate of the order ℓ, and define $\widehat{\boldsymbol{r}}^{(\ell)}$, $\widehat{\boldsymbol{Q}}^{(\ell)}$ and $\widehat{z}^{(\ell)}$ as the estimates of $\boldsymbol{r}$, $\boldsymbol{Q}$, and $\mathcal{Z}$, respectively, obtained by assuming $\mathcal{Z}$ is of order ℓ. The BIC is a penalized maximum likelihood estimator statistic [8], and the estimated order is computed as follows:

$$\widehat{\ell} = \underset{\ell \in \mathbb{N}}{\operatorname{argmin}} \left\{ -2 \ln L(\mathcal{Y} | \widehat{\boldsymbol{r}}^{(\ell)}, \widehat{\boldsymbol{Q}}^{(\ell)}, \widehat{z}^{(\ell)}) + \ell^2 \ln(N+1) \right\}. \tag{12}$$

The quantity ℓ^2 in the second term of (12) corresponds to the total number of parameters estimated by the MCMC procedure (ℓ elements of $\boldsymbol{r}$ and $\ell^2 - \ell$ off-diagonal elements of $\boldsymbol{Q}$), and $N+1$ is the total number of signal observations.

Finally, a procedure for estimating the mean signal path is presented. The mean signal path refers to the stochastic process $\{\widehat{Y}(t) : t \in [0, T]\}$, which is the estimate of the signal process $\{Y(t) : t \in [0, T]\}$ obtained by using $\widehat{\boldsymbol{r}}$, $\widehat{\boldsymbol{Q}}$, and $\widehat{z}$. That is, using a forward-filtering, backward smoothing algorithm, we estimate the likelihood that the environment occupies one of its estimated $\widehat{\ell}$ states in the time intervals between estimated environment transition times. The mean signal path is then constructed by weighting the degradation rates by their respective likelihoods to obtain the mean degradation rate in each time interval and, subsequently, computing the cumulative degradation accrued from these rates. This estimate can be used to assess the quality of parameter estimates by comparing $\widehat{Y}(t)$ with the true signal path.

Let M be the estimated total number of transitions in $\widehat{z}$ during $[0,T]$, and let the ordered sets $\{i_0, i_1, \ldots, i_M\}$ and $\{s_1, s_2, \ldots, s_M\}$ denote, respectively, the state sequence and transition times of $\widehat{z}$, where $i_0, i_1, \ldots, i_M \in \mathcal{S}$ and $s_1, s_2, \ldots s_M \in [0,T]$. Denote by $\Delta\widehat{Y}_m \equiv \mathbb{E}[Y(s_m) - Y(s_{m-1})]$ the expected increment of Y on $[s_{m-1}, s_m]$, where

$$\Delta\widehat{Y}_m = \sum_{i=1}^{\widehat{\ell}} r_i(s_m - s_{m-1})\mathbb{P}(Z_{m-1} = i|\mathcal{Y}, \widehat{\boldsymbol{r}}, \widehat{\boldsymbol{Q}}), \quad m = 1, 2, \ldots, M.$$

Using $\Delta\widehat{Y}_m$, $m = 1, 2, \ldots, M$, we can compute

$$\widehat{Y}(t) = (t - s_\kappa)\Delta\widehat{Y}_{\kappa+1} + \sum_{i=1}^{\kappa} \Delta\widehat{Y}_m, \quad t \in [0,T],$$

where $\kappa \equiv \max\{m \geq 1 : s_m \leq t\}$. Computing $\Delta\widehat{Y}_m$ requires that $\mathbb{P}(Z_m = i|\mathcal{Y}, \widehat{\boldsymbol{r}}, \widehat{\boldsymbol{Q}})$ be determined for all $i = 1, 2, \ldots, \widehat{\ell}$ and $m = 0, 1, \ldots, M$. These conditional probabilities are estimated by applying a *forward-filtering-backward-smoothing* (FFBS) algorithm to $\widehat{z}$ using $\widehat{\boldsymbol{Q}}$ and $\widehat{\boldsymbol{r}}$. Let $\mathcal{Y}^{(m)} \equiv \{Y(t_j) : t_j \leq s_m\}$ be the set of data observed up to time s_m, $m = 1, 2, \ldots, M$, and define a piecewise-linear function $Y^{(m)}(t)$ on $[0, s_m]$ such that $Y^{(m)}(t) = Y(t)$ for $t \in [0, s_m]$ and is zero otherwise. Lastly, for $m = 1, 2, \ldots, M$, let

$$\begin{aligned} f(Y(s_m)|Z_m = i, \mathcal{Y}^{(m-1)}, \widehat{\boldsymbol{r}}, \widehat{\boldsymbol{Q}}) &= \exp\left[\frac{\widehat{r}_i}{\widehat{\sigma}^2}\int_{s_{m-1}}^{s_m} \mathrm{d}Y^{(m)}(u) - \frac{\widehat{r}_i^2}{2\widehat{\sigma}^2}\int_{s_{m-1}}^{s_m} \mathrm{d}u\right] \\ &= \exp\left\{\frac{\widehat{r}_i}{\widehat{\sigma}^2}\left[Y^{(m)}(s_m) - Y^{(m)}(s_{m-1})\right] - \frac{\widehat{r}_i^2}{2\widehat{\sigma}^2}(s_m - s_{m-1})\right\} \end{aligned}$$

be the conditional density of the observation $Y(s_m)$ at time s_m, given observations $\mathcal{Y}^{(m-1)}$, $Z(m) = i$, and estimated parameters $\widehat{\boldsymbol{r}}$ and $\widehat{\boldsymbol{Q}}$. Next, the filtering and smoothing procedures are described in greater detail.

The objective of the filtering procedure, originally developed in [5], is to compute $\mathbb{P}(Z_m = i|\mathcal{Y}^{(m)}, \widehat{\boldsymbol{r}}, \widehat{\boldsymbol{Q}})$, for $i = 1, 2, \ldots, \widehat{\ell}$ and $m = 1, 2, \ldots, M$. This probability is computed recursively for $m = 1, 2, \ldots, M$ as follows:

1. For $i = 1, 2, \ldots, \widehat{\ell}$, compute $\mathbb{P}(Z_m = i|\mathcal{Y}^{(m-1)}, \widehat{\boldsymbol{r}}, \widehat{\boldsymbol{Q}})$, the one-step ahead prediction probabilities for Z_m, where

$$\begin{aligned} \mathbb{P}(Z_m = i|\mathcal{Y}^{(m-1)}, \widehat{\boldsymbol{r}}, \widehat{\boldsymbol{Q}}) &= \sum_{j=1}^{\widehat{\ell}} \hat{p}_{ji}\mathbb{P}(Z_{m-1} = j|\mathcal{Y}^{(m-1)}, \widehat{\boldsymbol{r}}, \widehat{\boldsymbol{Q}}), \qquad (13) \\ \hat{p}_{ji} &= \begin{cases} -\hat{q}_{ji}/\hat{q}_{jj}, & j \neq i, \\ 0, & j = i, \end{cases} \end{aligned}$$

   and $\mathbb{P}(Z_0 = i|\mathcal{Y}^{(0)}, \widehat{\boldsymbol{r}}, \widehat{\boldsymbol{Q}}) = 1/\widehat{\ell}$.

2. Compute the filtered probabilities $\mathbb{P}(Z_m = i|\mathcal{Y}^{(m)}, \widehat{\boldsymbol{r}}, \widehat{\boldsymbol{Q}})$ for $i = 1, 2, \ldots, \widehat{\ell}$, using (13), where

$$\mathbb{P}(Z_m = i|\mathcal{Y}^{(m)}, \widehat{\boldsymbol{r}}, \widehat{\boldsymbol{Q}}) = \frac{f(Y(s_m)|Z_m = i, \mathcal{Y}^{(m-1)}, \widehat{\boldsymbol{r}}, \widehat{\boldsymbol{Q}})\mathbb{P}(Z_m = i|\mathcal{Y}^{(m-1)}, \widehat{\boldsymbol{r}}, \widehat{\boldsymbol{Q}})}{\sum_{j=1}^{\widehat{\ell}} f(Y(s_m)|Z_m = j, \mathcal{Y}^{(m-1)}, \widehat{\boldsymbol{r}}, \widehat{\boldsymbol{Q}})\mathbb{P}(Z_m = j|\mathcal{Y}^{(m-1)}, \widehat{\boldsymbol{r}}, \widehat{\boldsymbol{Q}})}. \quad (14)$$

The filtered probabilities $\mathbb{P}(Z_m = i|\mathcal{Y}^{(m)}, \widehat{\boldsymbol{r}}, \widehat{\boldsymbol{Q}})$ from (14) are then used in the smoothing procedure, to compute $\mathbb{P}(Z_m = i|\mathcal{Y}, \widehat{\boldsymbol{r}}, \widehat{\boldsymbol{Q}})$, $i \in \mathcal{S}$, iteratively backward in time for $m = M-1, M-2, \ldots, 1$ as follows:

$$\mathbb{P}(Z_m = i|\mathcal{Y}, \widehat{\boldsymbol{r}}, \widehat{\boldsymbol{Q}}) = \sum_{j=1}^{\widehat{\ell}} \frac{\hat{p}_{ij}\,\mathbb{P}(Z_m = i|\mathcal{Y}^{(m)}, \widehat{\boldsymbol{r}}, \widehat{\boldsymbol{Q}})\mathbb{P}(Z_{m+1} = j|\mathcal{Y}, \widehat{\boldsymbol{r}}, \widehat{\boldsymbol{Q}})}{\sum_{k=1}^{\widehat{\ell}} \hat{p}_{kj}\mathbb{P}(Z_m = k|\mathcal{Y}^{(m)}, \widehat{\boldsymbol{r}}, \widehat{\boldsymbol{Q}})}, \quad (15)$$

where $\mathbb{P}(Z_M = i|\mathcal{Y}, \widehat{\boldsymbol{r}}, \widehat{\boldsymbol{Q}})$ is obtained from (14) with $m = M$ (see [12]). The initial distribution, $\mathbb{P}(Z_0 = i|\mathcal{Y}, \widehat{\boldsymbol{r}}, \widehat{\boldsymbol{Q}})$ can be obtained by continuing computation of (15) to $m = 0$, and setting $\widehat{\boldsymbol{\alpha}} = \mathbb{P}(Z_0 = i|\mathcal{Y}, \widehat{\boldsymbol{r}}, \widehat{\boldsymbol{Q}})$.

In the next section, numerical examples illustrating our modeling framework and the performance of the MCMC procedure are presented for both simulated and real degradation processes. These examples highlight the diversity of environment-driven degradation processes that can be estimated using this approach.

4 Numerical Results

In this section, the degradation model and inference procedure for estimating component lifetimes are illustrated using simulated and real degradation data. In each case, the estimated environment parameters are obtained by sampling signals up to various percentages of their threshold first passage time, and those estimates are used to compute the expected lifetime. These lifetime estimates are then compared to the actual component failure times (first passage times to the critical threshold, x).

4.1 Examples Using Simulated Data

For Examples 1 and 2 that follow, we generated 100 signal sample paths of $\{Y(t) : t \geq 0\}$ in accordance with the type of environment process assumed in each case. The signals were allowed to evolve up to a fixed threshold x units, at which time the component is declared to be failed. Let $T_n(x)$ denote the crossing time of the nth simulated path, $n = 1, 2, \ldots, 100$. Each path was observed up to p-percent of its crossing time, where $p \in \{25, 50, 75, 90\}$. Let $t_n^p \equiv p \times T_n(x)/100$ denote the time corresponding to p percent of the nth component's lifetime. For each (n, p), we set $\mathcal{T}_p^{(n)} = \{t_j : t_j \leq t_n^p\}$ and $\mathcal{Y}_p^{(n)} = \{Y(t_j) : t_j \in \mathcal{T}_p^{(n)}\}$ to obtain $(\widehat{\boldsymbol{r}}, \widehat{\boldsymbol{Q}}, \widehat{z})$ using the MCMC

procedure. The expected lifetime, denoted by τ_n^p, is then computed using (2) and (4). The quality of the estimates is assessed by computing the percent absolute error, $\epsilon_p^{(n)}$, given by

$$\epsilon_p^{(n)} = \frac{|\tau_n^p - T_n(x)|}{T_n(x)} \times 100. \tag{16}$$

Because we simulate 100 sample paths, box plots are used to display the variability in results. A similar procedure is applied to the real degradation data, except that have at our disposal only a limited number of paths with which comparisons can be made. We first consider the case in which the environment is actually a CTMC and the degradation accumulates as per equation (8).

Example 1: A CTMC Environment. Consider a component evolving in a three-state, CTMC environment with generator matrix $\boldsymbol{Q}$ and degradation rate vector $\boldsymbol{r}$ given in the left-hand column of Table 1. For this example, the critical degradation threshold is assumed to be $x = 1000$ units and $\sigma = 0.316$. Figure 1 depicts one of the 100 simulated degradation paths, along with the

Table 1: Quality of environment and degradation rate estimates.

True Parameter	Estimate of True Parameter
$\boldsymbol{Q} = \begin{bmatrix} -1.0 & 0.5 & 0.5 \\ 0.75 & -1.5 & 0.75 \\ 1.0 & 1.0 & -2.0 \end{bmatrix}$	$\widehat{\boldsymbol{Q}} = \begin{bmatrix} -0.8190 & 0.4784 & 0.3406 \\ 0.7550 & -1.5112 & 0.7561 \\ 0.7037 & 0.8709 & -1.5745 \end{bmatrix}$
$\boldsymbol{r} = \begin{bmatrix} 1 & 5 & 10 \end{bmatrix}$	$\widehat{\boldsymbol{r}} = \begin{bmatrix} 1.1046 & 4.8863 & 9.6783 \end{bmatrix}$
$\ell = 3$	$\hat{\ell} = 3$

estimated mean path generated using the FFBS algorithm described in section 3. The true path was observed at $N = 23,466$ discrete times, and estimates of the environment parameters, $\widehat{\boldsymbol{Q}}$ and $\widehat{\boldsymbol{r}}$, obtained via the MCMC procedure of section 3, are given in Table 1. The BIC-estimated order of the environment process is $\hat{\ell} = 3$ (i.e., $\mathcal{S} = \{1, 2, 3\}$). The close correspondence of the observed and mean signal paths suggests that the estimates $(\widehat{\boldsymbol{r}}, \widehat{\boldsymbol{Q}}, \widehat{z})$ characterize the signal process and crossing time very well. This conclusion is corroborated by Figure 2, which shows box plots of the percent absolute error of estimated lifetimes for each p. The plots indicate that both the median and variance of absolute error tend to decrease as p increases. Although the absolute error can be large (as evidenced by an outlier above 25%), the fact that the median absolute error is well below 10% indicates the procedure provides reasonable estimates of expected lifetime when the environment process is a CTMC.

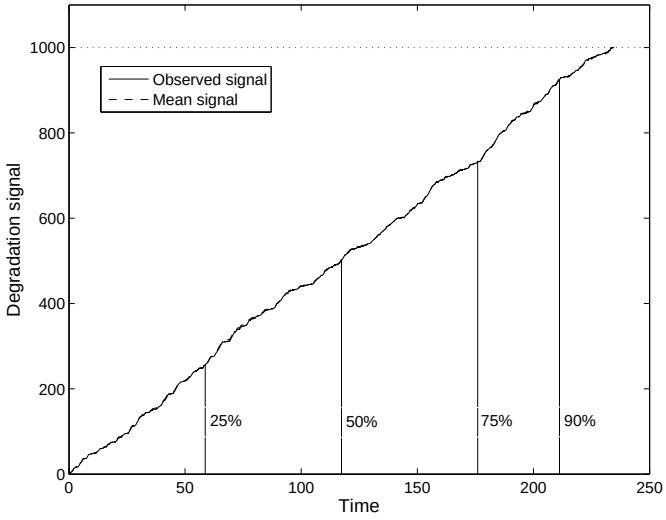

Figure 1: Observed and mean signal paths (CTMC environment).

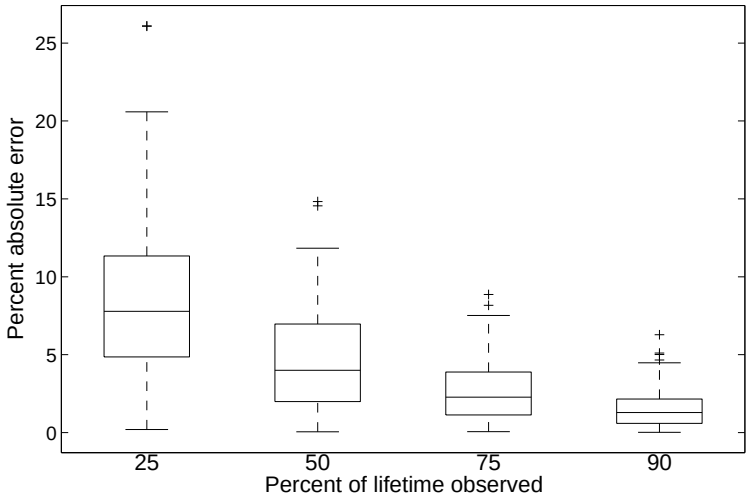

Figure 2: Box plot of percent absolute error (CTMC environment).

Example 2: A Semi-Markov Environment. Consider now a finite semi-Markov environment whose inter-transition times are not memoryless. Signal paths were generated for two distinct cases: (a) $\ell = 10$ states, and (b) $\ell = 20$ states. The transition probabilities, as well as the holding times and degradation rates for each environment state, were randomly generated according to Table 2, where $[\nu_1, \nu_2, \nu_3] \sim U(0,1)^3$ such that $\nu_1 < \nu_2 < \nu_3$, $\nu_4 = 0.1 + 3.0\,U(0,1)$ and $\nu_5 = 0.1 + 3.0\,U(0,1)$, where $U(0,1)$ is a continuous uniform random variable with support $[0,1]$.

Table 2: Summary of holding-time distributions and degradation rates.

State index	Holding Time Distribution	Degradation Rate
1,4,7,9,12,15,19,20	Uniform$(0,1)$	Uniform$(0,2)$
2,10,13,16	Triangle(ν_1,ν_2,ν_3)	Uniform$(0,2)$
3,6,14,17	Gamma$(0.5,0.5)$	20
5,8,11,19	Beta(ν_4,ν_5)	Uniform$(0,2)$

A key feature of these environments is that signal paths tend to have sudden increases in growth due to the relatively high degradation rate and potentially long holding times associated with the Gamma-distributed states. Each signal path is simulated with a diffusion coefficient of $\sigma = 0.707$ and observed at equidistant times $t_j - t_{j-1} = 0.01$, $j = 1, 2, \ldots, N$. Failure is assumed when the signal reaches a threshold $x = 3000$ and $\sigma = 0.707$. Figures 3 and 5 show simulated signal paths observed at $N = 88,050$ and $N = 99,863$ discrete times for $\ell = 10$ and $\ell = 20$, respectively. The estimated number of states obtained by observing a single signal path from each environment are $\hat{\ell}_{10} = 3$ and $\hat{\ell}_{20} = 2$ for the 10- and 20-state cases, respectively. Although, for this example, it is counterintuitive that the estimated number of states decreases as the true number of environment states increases, this behavior can be attributed to the fact that most of the states have associated degradation rates that are uniformly distributed on the interval $[0,2]$. Consequently, it may be difficult for the procedure to distinguish between these states; therefore, $\hat{\ell}$ is relatively small, despite the large number of true environment states. Estimates of the environment parameters obtained from each signal path are as follows:

$$\widehat{\boldsymbol{Q}}_{10} = \begin{bmatrix} -0.0795 & 0.0511 & 0.0284 \\ 0.1585 & -0.2661 & 0.1076 \\ 0.2322 & 0.1906 & -0.4229 \end{bmatrix} \quad \widehat{\boldsymbol{r}}_{10} = \begin{bmatrix} 2.1408 & 4.8024 & 9.4680 \end{bmatrix},$$

$$\widehat{\boldsymbol{Q}}_{20} = \begin{bmatrix} -0.0841 & 0.0841 \\ 0.4275 & -0.4275 \end{bmatrix} \quad \widehat{\boldsymbol{r}}_{20} = \begin{bmatrix} 1.9587 & 8.4067 \end{bmatrix}.$$

Comparing the mean signal paths with the observed paths in Figures 3 and 5 indicates that the parameters obtained using relatively small BIC-estimated orders adequately characterize the signal processes, despite the fact that the true environment processes are non-Markovian with 10 and 20

states, respectively.

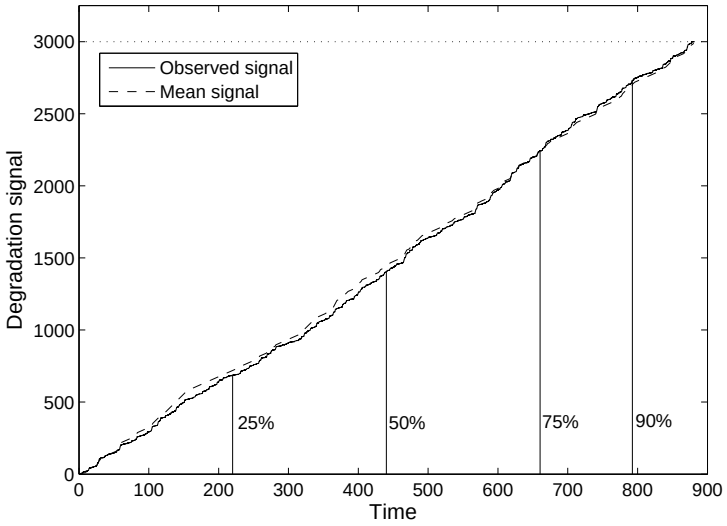

Figure 3: Observed and mean signal paths ($\ell = 10$ semi-Markov environment).

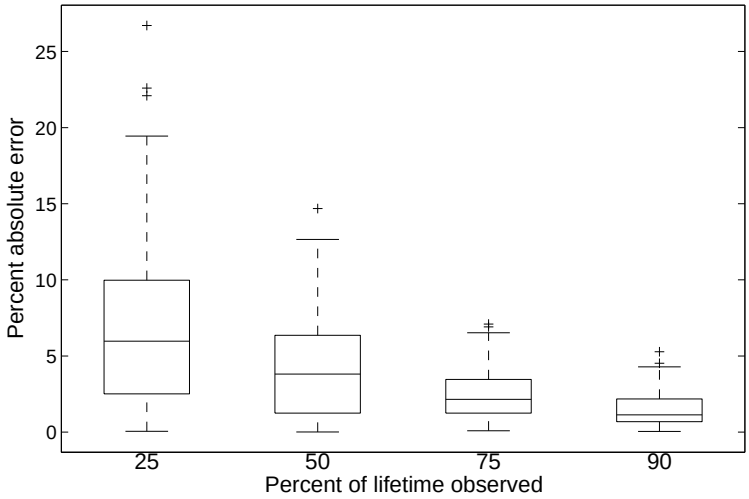

Figure 4: Box plot of percent absolute error ($\ell = 10$ semi-Markov environment).

One hundred simulated signal paths were generated for each environment and observed up to p percent of their respective failure times, $p \in \{25, 50, 75, 90\}$. Figures 4 and 6 show box plots of percent absolute error for each p in the 10- and 20-state cases, respectively. Interestingly, the median errors in the semi-Markov cases are consistent with those in the CTMC case (see Figure 2). Moreover, the dispersion of errors in the semi-Markov cases is consistent with the irregularity induced by the Gamma-distributed state holding times. As in the CTMC case, the median absolute error and variance decrease rapidly as the proportion of lifetime observed (p) increases. The median absolute error is below 5% in both cases when only 50% of the lifetime has been observed.

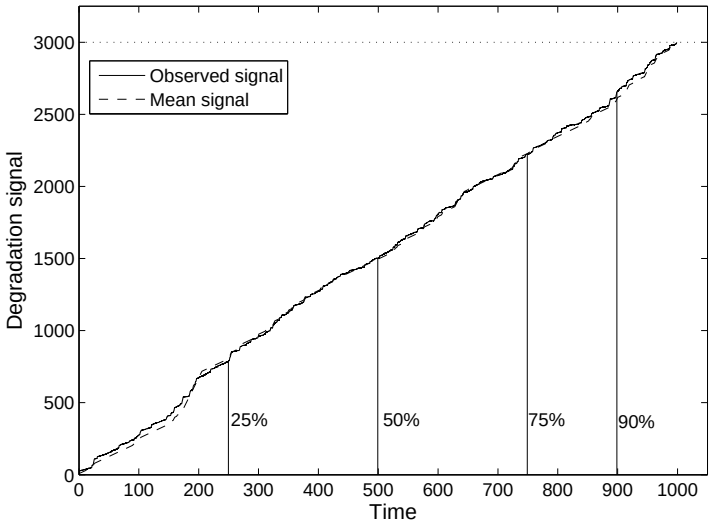

Figure 5: Observed and mean signal paths ($\ell = 20$ semi-Markov environment).

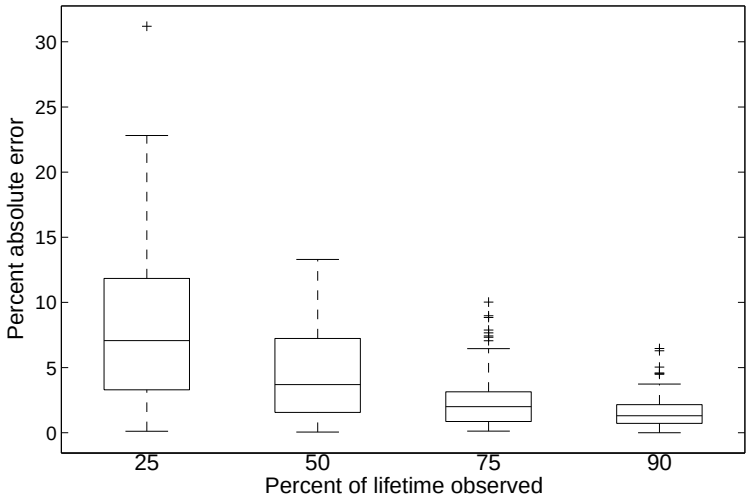

Figure 6: Box plot of percent absolute error ($\ell = 20$ semi-Markov environment).

4.2 Examples Using Real Degradation Data

In this subsection, we validate the estimation procedure using real degradation data. There are three separate cases: (1) fatigue crack length data; (2) thrust bearing vibration data; and (3) wind turbine gear degradation.

Example 3: Fatigue Crack Length. First, we illustrate the procedure using experimental data originally published by Virkler *et al.* [49]. The data contain measurements of the growth of a fatigue crack over time (as measured by the number of load cycles) for 68 specimens of 2024-T3 aluminum alloy. Representative sample paths are depicted in Figure 7, and specimen failure is assumed to occur when the crack length exceeds 45 mm. The curvature in the sample paths suggests an exponential relationship between the crack length and the number of load cycles, clearly violating the assumption that the degradation "signal" evolves according to (7). The MCMC procedure of

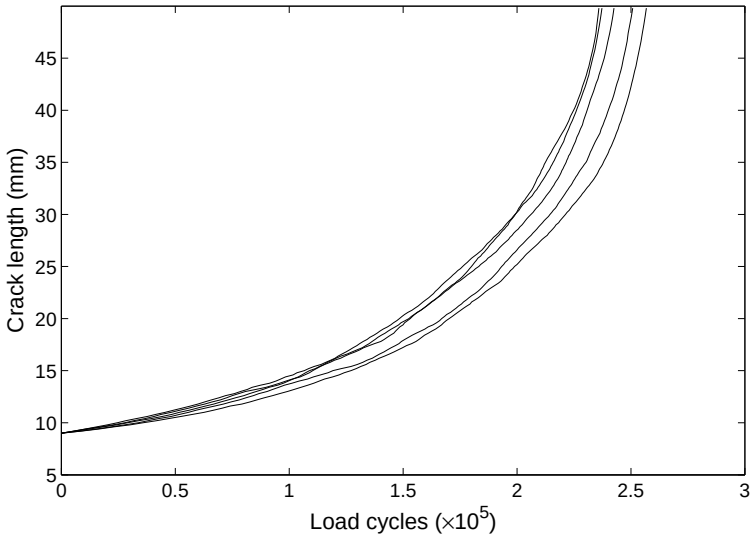

Figure 7: Sample paths of fatigue crack length propagation.

section 3 was applied to the log-transformed sample paths of crack lengths as the transformed paths exhibit milder curvature than the untransformed paths. We pause here to make an important point. Extensive empirical testing has shown that the MCMC procedure can perform poorly for signals that do not evolve as a switching diffusion model when $\sigma \leq \sqrt{10}$. For this reason, the transformed crack lengths, and the transformed threshold, were multiplied by a factor of 100 before applying the MCMC procedure. All transformed paths were translated to begin at the origin.

To evaluate performance, path observations are restricted to $p \in \{75, 90, 100\}$ as the curvature is not strongly apparent until $p > 50$. Furthermore, it is possible that one or more elements in $\widehat{\boldsymbol{r}}$ are not strictly positive due to the relatively long regime of nearly flat crack growth. If $\widehat{\boldsymbol{r}} \not> \mathbf{0}$ then equations (2) and (4) cannot be used with the estimates $\widehat{\boldsymbol{Q}}$ and $\widehat{\boldsymbol{r}}$ to approximate the expected lifetimes. Alternatively, expected lifetimes were computed using the asymptotic result (5).

Figure 8 shows one of the transformed sample paths and its corresponding mean path. The BIC-estimated number of environment states for this degradation process was estimated using only this single path, and the estimate is $\hat{\ell} = 2$. Although the evolution of the true degradation sample path deviates significantly from that of a switching diffusion model, it can still be well characterized using the estimated model parameters. A box plot of the percent absolute error is shown in Figure 9 for all 68 sample paths observed up to each respective p. For $p = 75$, $p = 90$ and $p = 100$,

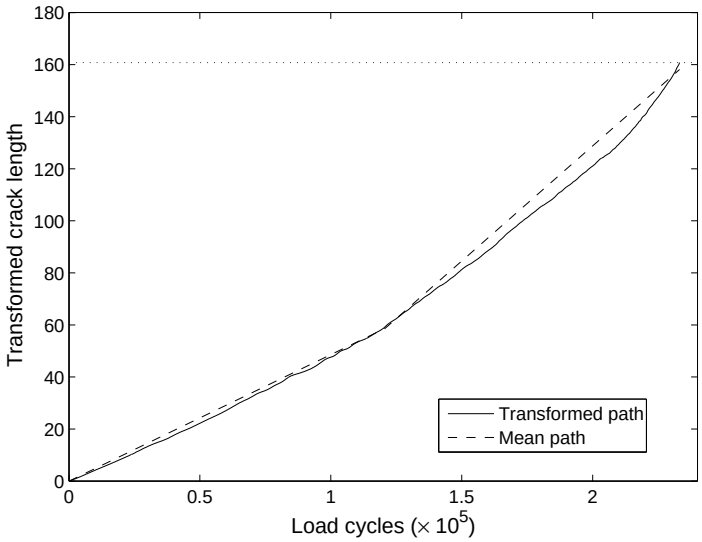

Figure 8: Observed and mean signal paths (crack-length data).

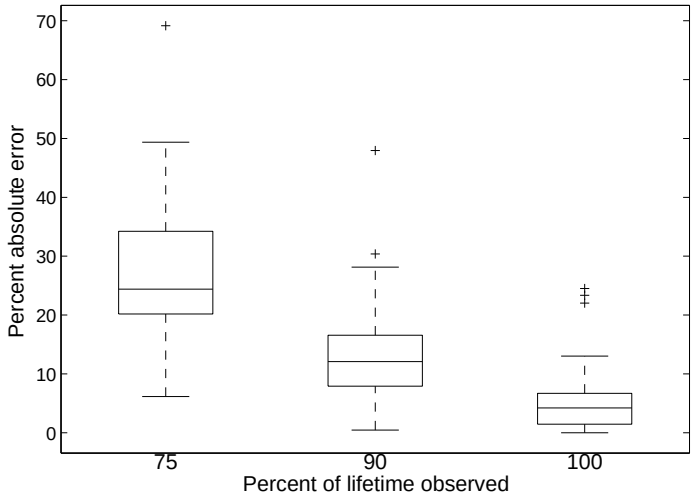

Figure 9: Box plot of percent absolute error (crack-length data).

the median absolute errors are 24.4%, 12.1%, and 4.2%, respectively, while the error variance exhibits a decreasing trend as p increases. The plots indicate that the MCMC procedure can provide reasonable estimates of lifetime in a fatigue crack length application, provided a sufficiently large

percentage of the lifetime is observed.

Example 4: Bearing Vibration Signal. In this example, the procedure is shown to effectively predict a bearing lifetime using vibration data. The vibration data were collected by Gebraeel and Pan [20] for 25 bearings tested until failure under constant loading and rotational conditions. Figure 10 shows the vibration signal for a single bearing. The vibration signals were collected at

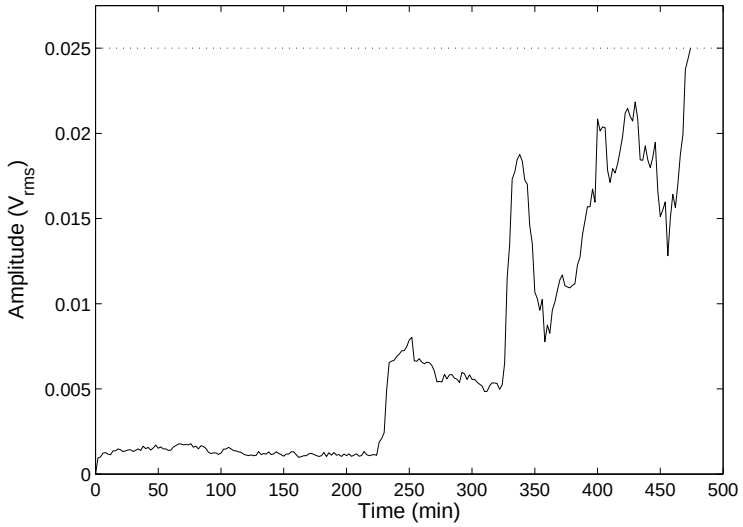

Figure 10: A vibration signal path.

2-minute intervals and represent the average amplitude over time of the defective bearing frequency and its first six harmonics. The threshold for bearing failure is based on the root mean square (rms) of the vibration amplitude, defined here as $0.025V_{\text{rms}}$. This vibration level corresponds to 2.2 Gs of acceleration and is consistent with the danger-level specification of 2.0–2.2 Gs in ISO 2372, the industrial standards for machinery vibration. Of the 25 bearings tested, one signal did not reach the threshold and was not considered.

Characteristic of the vibration signals is an initial period at which the amplitude is relatively constant with only small oscillations due to random noise. After some time, the signals experience a sudden upward jump after which they exhibit larger oscillations and an increasing trend until failure. The vibration signals clearly do not satisfy the assumption of model (7) that σ is independent of time. The bearing lifetimes are only predicted from the instant at which the vibration signal exhibits its first large jump until it reaches the critical threshold x. The vibration signals were transformed in a manner similar to that of the Virker data of Example 3. To dampen the signal oscillations, inference was performed on log-transformed amplitudes which were multiplied by a factor of 10^3 to increase $\widehat{\sigma}$ to an appropriate magnitude for adequate performance of the MCMC procedure. All paths were translated to begin at the origin. For each path, at least one element of $\widehat{\boldsymbol{r}}$ is negative; therefore, the expected lifetimes were estimated using the asymptotic result of (5). The BIC-estimated number of environment states obtained by observing a single bearing vibration

signal is $\hat{\ell} = 3$.

Figure 11 shows a plot of one of the vibration paths (untransformed) and the corresponding mean signal path. The close correspondence of the paths indicates that parameter estimates are obtained that characterize the vibration process well. Box plots of percent absolute error for all 24 paths observed at $p \in \{50, 75, 90\}$ are shown in Figure 12.

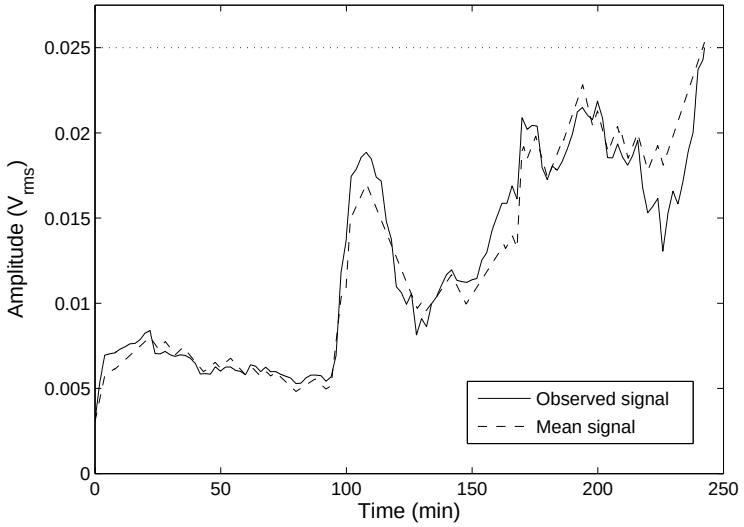

Figure 11: Observed and mean signal paths (vibration data).

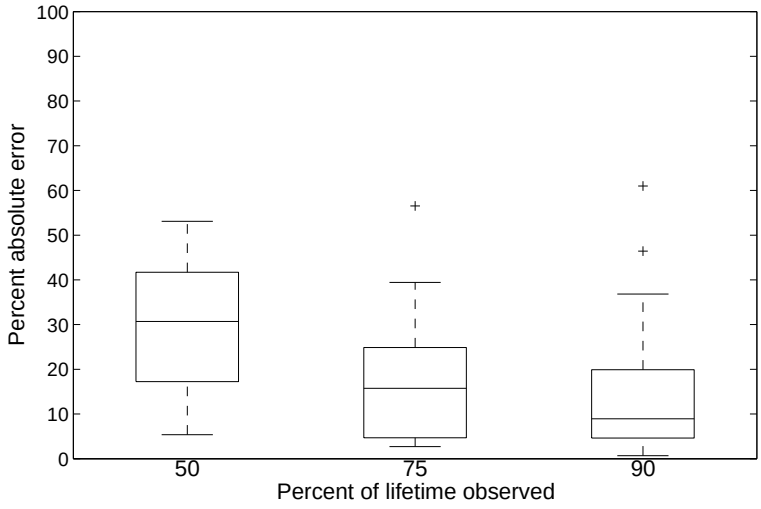

Figure 12: Box plot of percent absolute error (vibration data).

It is noted that the median absolute error decreases monotonically in p while the variance is fairly constant over the range of p values. There are two important points to make here: (1) the estimated mean signal tracks the observed signal remarkably well; and (2) although no information is provided about the environment, we are able to characterize the evolution of the degradation

signal using the switching diffusion model.

Example 5: Wind Turbine Gear Degradation. This case considers lifetime prediction for a gear that operates in a wind turbine's drivetrain. The signal for gear wear will correspond to the effective number of load cycles and is computed from explicit field observations of shaft torque and rotor speed. The measurements are from a proprietary data set collected for a single wind turbine over a 19-month period that consists of 10-minute summary statistics. That is, for each 10-minute interval, descriptive statistics (including the mean, minimum, maximum, standard deviation, etc.) were obtained for each turbine parameter. After discarding intervals for which data are missing (due to downtime or other causes), summary statistics of turbine torque and rotor speed are available for 12,067 time periods. The failure threshold is defined as the effective number of load cycles at which a gear tooth will fail.

Let ζ_i and ω_i denote the mean torque (ft-lbs) and rotor speed (rpm) of the wind turbine over the ith time period, $i = 1, 2, \ldots, N = 12,067$. To relate these parameters to the effective number of load cycles imposed on the gear tooth, recall that the relationship between torque and gear stress, denoted by ξ, can be approximated as

$$\xi = h\zeta,$$

where $h > 0$ is a constant [47]. Let ξ_w denote the stress amplitude corresponding to w cycles on a stress-life (S-N) curve of the gear material, and $(w', \xi_{w'})$ denote another known point on the S-N curve. The function $n(\xi)$, defined as the number of cycles to failure under stress amplitude ξ, is approximated by a power law as follows [42]:

$$n(\xi) = w(\xi/\xi_w)^{1/b}$$

where the parameter b is given by

$$b = -\frac{\ln(\xi_w/\xi_{w'})}{\ln(w'/w)}.$$

For stress amplitude ξ, let $\tilde{n}(\xi) \equiv w/n(\xi)$ be the effective number of load cycles imposed on a gear tooth during one cycle of amplitude ξ. Assuming a gear tooth experiences c load cycles per revolution, the total effective number of load cycles during the ith 10-minute period, denoted η_i, is approximately

$$\eta_i = 10\, c\, \omega_i\, \tilde{n}(\xi_i).$$

The signal value at t_i is computed in a straightforward way as

$$Y(t_i) = \sum_{j=1}^{i} \eta_j, \quad i = 0, 1, 2, \ldots, N, \tag{17}$$

where $Y(0) \equiv 0$.

In this example, $h = c = 1$, $w = 10^7$, and $\xi_w = 63.0$ (a value close to the overall mean torque observed in the data). Three S-N curves were considered based on different values of $(w', \xi_{w'})$: Case

(a) $(100, 0.3 \times 10^7)$, Case (b) $(100, 0.5 \times 10^6)$, and Case (c) $(100, 0.1 \times 10^6)$. Note that in progressing from Case (a) to Case (c), the total effective number of load cycles imposed on the material increases for each fixed $\xi > \xi_w$. Signal paths were computed using a bootstrap technique whereby the torque and rotor speed values are generated by randomly sampling 4-hour, contiguous blocks of torque and rotor speed data. The failure threshold was assumed to be $x = 10^7$. The estimated number of environment states are $\hat{\ell} = 2$, $\hat{\ell} = 2$, and $\hat{\ell} = 3$ for Cases (a), (b) and (c), respectively. Figures 13, 15, and 17 show the observed signals used to compute the BIC statistic for Cases (a), (b), and (c), respectively, along with the mean signal paths obtained from the estimated parameters corresponding to each path. That the mean and observed signal paths correspond closely for all three cases indicates that the degradation process for the gear tooth is well characterized by the estimated parameters.

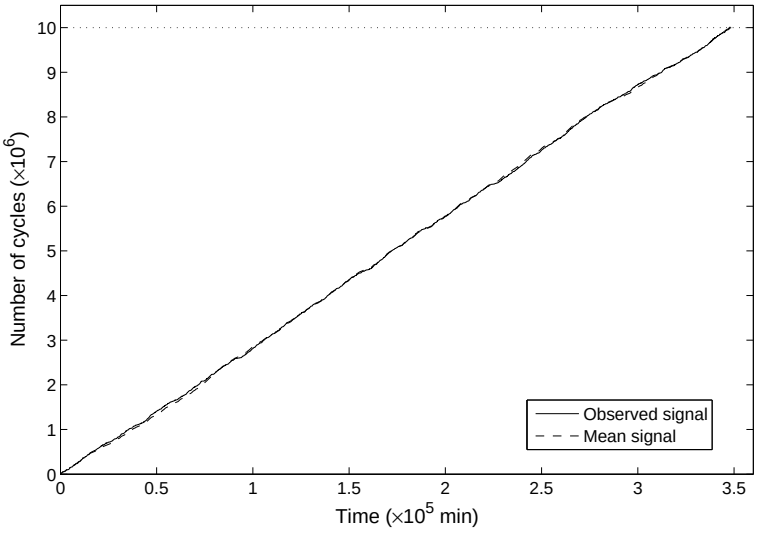

Figure 13: Observed and mean signal paths: Gear tooth degradation Case (a).

Figures 14, 16, and 18 show box plots of the percent absolute error for Cases (a), (b), and (c), respectively, with 100 randomly generated signal paths observed up to p percent of their respective failure times, $p \in \{25, 50, 75, 90\}$. For fixed p, the median and variance of the absolute error increases from Case (a) to Case (c) – an intuitive result as Cases (b) and (c) can have relatively large degradation rates leading to more irregular sample paths. For Case (a), the most realistic case in a practical application, the median absolute error is less than 5% for all p, and for Cases (b) and (c), the median absolute error is below 10% and 20%, respectively, for all p. That the inference procedure also performs well in the more extreme Cases (b) and (c) suggests that the procedure is well-suited to estimate the lifetimes of gears that operate in relatively extreme degradation environments.

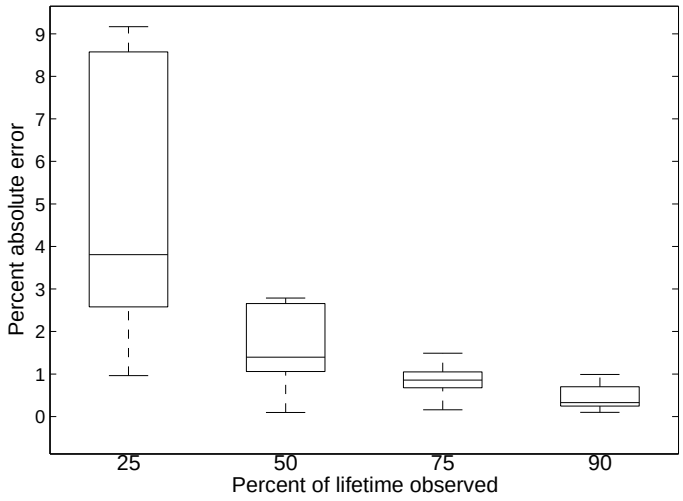

Figure 14: Box plot of percent absolute error: Gear tooth degradation Case (a).

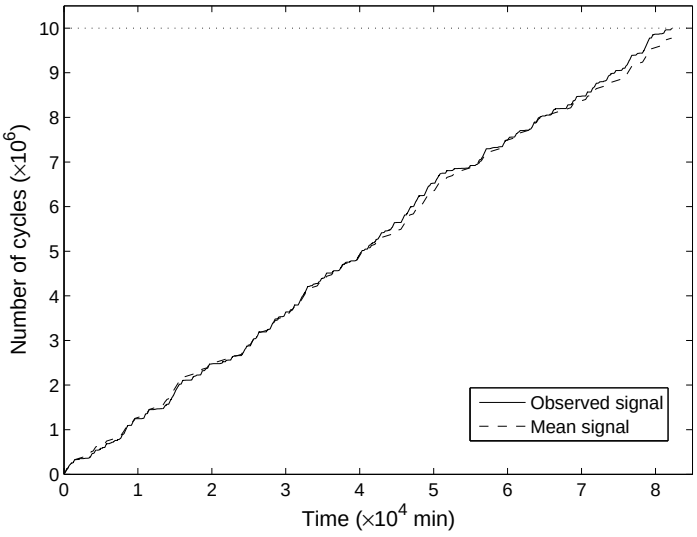

Figure 15: Observed and mean signal paths: Gear tooth degradation Case (b).

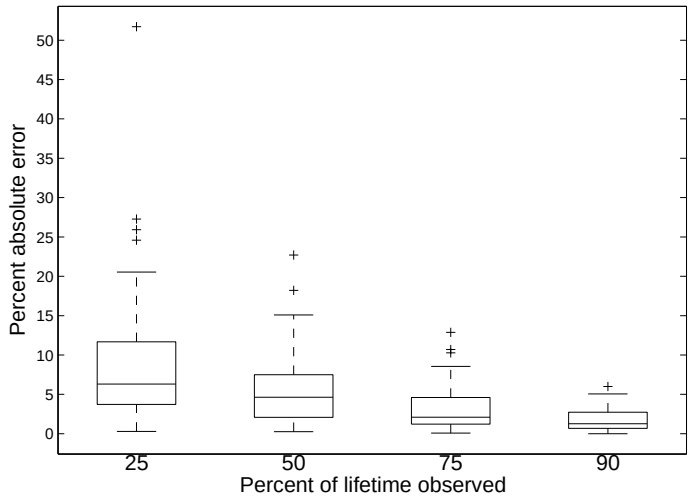

Figure 16: Box plot of percent absolute error: Gear tooth degradation Case (b).

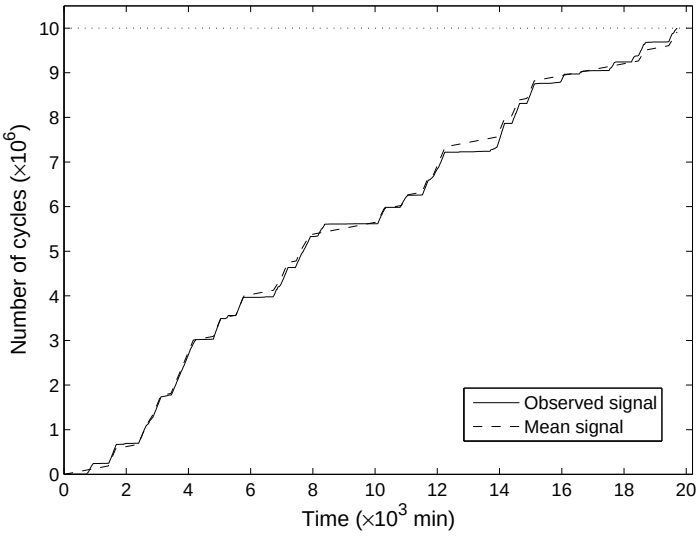

Figure 17: Observed and mean signal paths: Gear tooth degradation Case (c).

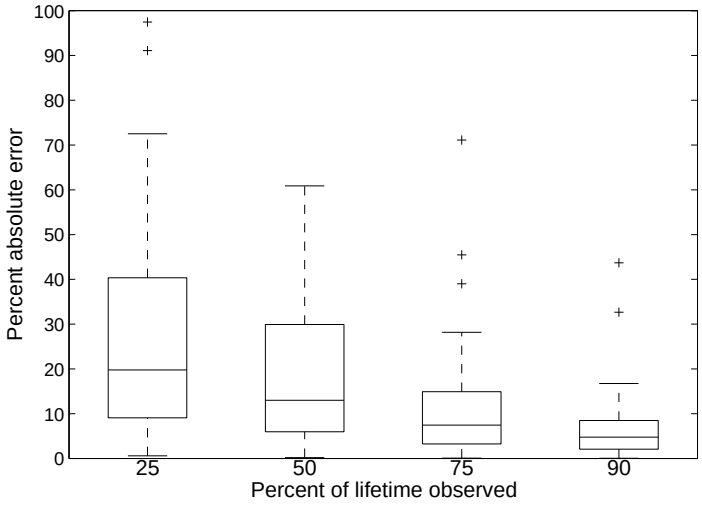

Figure 18: Box plot of percent absolute error: Gear tooth degradation Case (c).

5 Conclusions

In this paper, we have presented a hybrid analytical-statistical technique to approximate the stochastic, environment-driven, degradation process of a component using an observed signal of degradation. The signal was assumed to evolve as a switching diffusion process, and the environment parameters were estimated using a Markov chain Monte Carlo statistical procedure. The performance of the technique was assessed by comparing the expected component lifetime and mean degradation signal obtained via the estimated environment parameters with the actual component lifetime and the observed degradation signal, respectively. Numerical results indicate that the framework is robust against signals that depart significantly from the stochastic behavior of a switching diffusion process. For degradation processes driven by non-Markovian environments, or those having non-constant degradation rates or time-nonhomogeneous variance, the framework was still able to characterize the degradation process well, provided that the signal observation period is sufficiently long.

Although the modeling frameworks described in sections 2 and 3 provide a viable approach to approximate the stochastic behavior of an arbitrary degradation process, they are limited by assumptions required for the switching diffusion model. In particular, when the variance of the degradation signal fluctuates significantly over non-overlapping time intervals, substantial preprocessing of the signal may be required to estimate the environment parameters. To more effectively handle such cases, the switching diffusion model should incorporate a time-nonhomogeneous diffusion coefficient, for which an appropriate inference procedure would be required. Similarly, the estimation procedure may not perform as well in applications where degradation signals evolve as nearly-deterministic, nonlinear functions of time and violate the assumption that the environment process is time-homogeneous (e.g., fatigue crack propagation). Although signal preprocessing can be helpful, a more realistic model should include degradation rates that are functions of time and/or the cumulative degradation level. Lastly, the MCMC statistical procedure does not easily facilitate real-time updating of the environment parameters as the signal is observed. In fact, there are no known filtering- or simulation-based procedures that are able to infer the parameters of a switching diffusion process in a real-time, iterative manner. Developing such an inference procedure would significantly reduce the computational burden and allow near-continuous updating of the model parameters as sensor data are collected.

Acknowledgements

The authors acknowledge, with gratitude, the helpful comments provided by three anonymous referees and the Associate Editor. This research was sponsored in part by two grants from the U.S. National Science Foundation (CMMI-0856192 and CMMI-0856702).

References

[1] J. Abate and W. Whitt. Numerical inversion of Laplace transforms of probability distributions. *ORSA Journal on Computing*, 7(1):36–43, 1995.

[2] M.S. Abdel-Hameed and F. Proschan. Nonstationary shock models. *Stochastic Processes and their Applications*, 1(4):383–404, 1973.

[3] D. Banjevic and A.K.S. Jardine. Calculation of reliability function and remaining useful life for a Markov failure time process. *IMA Journal of Management Mathematics*, 17(2):115–130, 2006.

[4] D. Banjevic, A.K.S. Jardine, V. Makis, and M. Ennis. A control-limit policy and software for condition-based maintenance optimization. *INFOR*, 39:32–50, 2001.

[5] E. Baum and T. Petrie. Statistical inference for probabilistic functions of finite state Markov chains. *The Annals of Mathematical Statistics*, 37(6):1554–1563, 1966.

[6] P. Billingsley. Statistical methods in Markov chains. *The Annals of Mathematical Statistics*, 32(1):12–40, 1961.

[7] P.G. Blackwell. Bayesian inference for Markov processes with diffusion and discrete components. *Biometrika*, 90(3):613–627, 2003.

[8] O. Cappé, E. Moulines, and R. Rydén. *Inference in Hidden Markov Models*. Springer, New York, NY, 2005.

[9] E. Çinlar. Markov additive processes II. *Z. Wahrscheinlichkeitstheorie verw. Geb.*, 24(2):95–121, 1972.

[10] E. Çinlar. Shock and wear models and Markov additive processes. In I.N. Shimi and C.P. Tsokos, editors, *The Theory and Applications of Reliability*, pages 193–214. Academic Press, New York, NY, 1977.

[11] J.H. Cha and J. Mi. Study of a stochastic failure model in a random environment. *Journal of applied probability*, 44(1):151–163, 2007.

[12] S. Chib. Calculating posterior distributions and model estimates in Markov mixuture models. *Journal of Econometrics*, 75(1):79–97, 1996.

[13] D.R. Cox. Regression models and life-tables. *Journal of the Royal Statistical Society. Series B (Methodological)*, 34(2):187–220, 1972.

[14] K.A. Doksum and A. Hóyland. Models for variable-stress accelerated life testing experiments based on Wiener processes and the inverse Gaussian distribution. *Technometrics*, 34(1):74–82, 1992.

[15] J.D. Esary, A.W. Marshall, and F. Prochan. Shock models and wear processes. *Annals of Probability*, 1(4):627–649, 1973.

[16] R.M. Feldman. Optimal replacement with semi-Markov shock models. *Journal of Applied Probability*, 13(1):108–117, 1976.

[17] D. Gamerman. Dynamic Bayesian models for survival data. *Applied Statistics*, 40(1):63–79, 1991.

[18] N. Gebraeel. Sensory-updated residual life distributions for components with exponential degradation patterns. *IEEE Transactions on Automation Science and Engineering*, 3(4):382–393, 2006.

[19] N. Gebraeel, M.A. Lawley, R. Li, and J.K. Ryan. Residual-life distributions from component degradation signals: A Bayesian approach. *IIE Transactions*, 37(6):543–557, 2005.

[20] N. Gebraeel and J. Pan. Prognostic degradation models for computing and updating residual life distributions in a time-varying environment. *IEEE Transactions on Reliability*, 57(4):539–550, 2008.

[21] A.E. Gelfand and A.F.M. Smith. Sampling-based approaches to calculating marginal densities. *Journal of the American Statistical Association*, 85(410):398–409, 1990.

[22] A. Ghasemi, S. Yacout, and M.S. Ouali. Evaluating the reliability function and the mean residual life for equipment with unobservable states. *IEEE Transactions on Reliability*, 59(1):45–54, 2010.

[23] M. Hahn, S. Frühwirth-Schnatter, and J. Sass. Markov chain Monte Carlo methods for parameter estimation in multidimension continuous time switching diffusion models. *Journal of Financial Econometrics*, 8(1):88–121, 2010.

[24] M. Hahn and J. Sass. Parameter estimation in continuous-time Markov switching models: A semi-continuous Markov chain Monte Carlo approach. *Bayesian Analysis*, 4(1):63–84, 2009.

[25] N. Igaki, U. Sumita, and M. Kowada. Analysis of Markov renewal shock models. *Journal of Applied Probability*, 32(3):821–831, 1995.

[26] A.K.S. Jardine, D. Banjevic, and V. Makis. Optimal replacement policy and the structure of software for condition-based maintenance. *Journal of Quality in Maintenance Engineering*, 3(2):109–119, 1997.

[27] J.P. Kharoufeh. Explicit results for wear processes in a Markovian environment. *Operations Research Letters*, 31(3):237–244, 2003.

[28] J.P. Kharoufeh and S.M. Cox. Stochastic models for degradation-based reliability. *IIE Transactions*, 37(6):533–542, 2005.

[29] J.P. Kharoufeh, D.E. Finkelstein, and D.G. Mixon. Availability of periodically inspected systems with Markovian wear and shocks. *Journal of Applied Probability*, 43(2):303–317, 2006.

[30] J.P. Kharoufeh and D.G. Mixon. On a Markov-modulated shock and wear process. *Naval Research Logistics*, 56(6):563–576, 2009.

[31] J.P. Kharoufeh, C.J. Solo, and M.Y. Ulukus. Semi-Markov models for degradation-based reliability. *IIE Transactions*, 42(8):599–612, 2010.

[32] M.L.T. Lee and G.A. Whitmore. Proportional hazards and threshold regression: Their theoretical and practical connections. *Lifetime Data Analysis*, 16(2):196–214, 2010.

[33] M.L.T. Lee, G.A. Whitmore, F. Laden, J.E. Hart, and E. Garshick. Assessing lung cancer risk in railroad workers using a first hitting time regression model. *Environmetrics*, 15(5):501–512, 2004.

[34] J. Leichty and G. Roberts. Markov chain Monte Carlo methods for switching diffusion models. *Biometrika*, 88(2):299–315, 2001.

[35] A.J. Lemoine and M.L. Wenocur. A note on shot-noise and reliability modeling. *Operations Research*, 34(2):320–323, 1986.

[36] C.M. Liao and S.T. Tseng. Optimal design for step-stress accelerated degradation tests. *IEEE Transactions on Reliability*, 55(1):59–66, 2006.

[37] H. Liao and E.A. Elsayed. Reliability inference for field conditions from accelerated degradation testing. *Naval Research Logistics*, 53(6):576–587, 2006.

[38] H. Liao and Z. Tian. A framework for predicting the remaining useful life of a single unit under time-varying operating conditions. *IIE Transactions*, 45(9):964–980, 2013.

[39] H. Liao, W. Zhao, and H. Guo. Predicting remaining useful life of an individual unit using proportional hazards model and logistic regression model. In *Annual Reliability and Maintainability Symposium*, pages 127–132, 2006.

[40] L.E. Myers. Survival functions induced by stochastic covariate processes. *Journal of Applied Probability*, 18(2):523–529, 1981.

[41] S. Özekici and R. Soyer. Bayesian analysis of Markov modulated Bernoulli processes. *Mathemathical Methods of Operations Research*, 57(1):125–140, 2003.

[42] J. Schijve. *Fatigue of Structures and Materials*. Springer, New York, NY, 2009.

[43] G. Schwartz. Estimating the dimension of a model. *The Annals of Statistics*, 6(2):461–464, 1978.

[44] X.S. Si, W. Wang, C.H. Hu, and D.H. Zhou. Remaining useful life estimation: A review on the statistical data driven approaches. *European Journal of Operational Research*, 213(1):1–14, 2011.

[45] N.D. Singpurwalla. Survival in dynamic environments. *Statistical Science*, 10(1):86–103, 1995.

[46] Y. Sun, L. Ma, J. Mathew, W. Wang, and S. Zhang. Mechanical systems hazard estimation using condition monitoring. *Mechanical Systems and Signal Processing*, 20(5):1189–1201, 2006.

[47] H.J. Sutherland and D.P. Burwinkle. The spectral content of the torque loads on a turbine gear tooth. *Wind Energy*, 16(1):91–97, 1995.

[48] S.T. Tseng, N. Balakrishnan, and C.C. Tsai. Optimal step-stress accelerated degradation test plan for Gamma degradation processes. *IEEE Transactions on Reliability*, 58(4):611–618, 2009.

[49] D.A. Virkler, B.M. Hilberry, and P.K. Goel. The statistical nature of fatigue crack propagation. *ASME Journal of Engineering Materials and Technology*, 101(2):148–153, 1979.

[50] P.J. Vlok, M. Wnek, and M. Zygmunt. Utilising statistical residual life estimates of bearings to quantify the influence of preventive maintenance actions. *Mechanical Systems and Signal Processing*, 18(4):833–847, 2004.

[51] G.A. Whitmore and F. Schenkelberg. Modelling accelerated degradation data using Wiener diffusion with a time scale transformation. *Lifetime Data Analysis*, 3(1):27–45, 1997.

[52] M.Y. You, L. Li, G. Meng, and J. Ni. Two-zone proportional hazard model for equipment remaining useful life prediction. *Journal of Manufacturing Science and Engineering*, 132(4):041008–1–041008–6, 2010.

[53] X. Zhao, M. Fouladirad, C. Bérenguer, and L. Bordes. Condition-based inspection/replacement policies for non-monotone deteriorating systems with environmental covariates. *Reliability Engineering and System Safety*, 95(8):921–934, 2010.